Journal of Materials Chemistry A

Accepted Manuscript

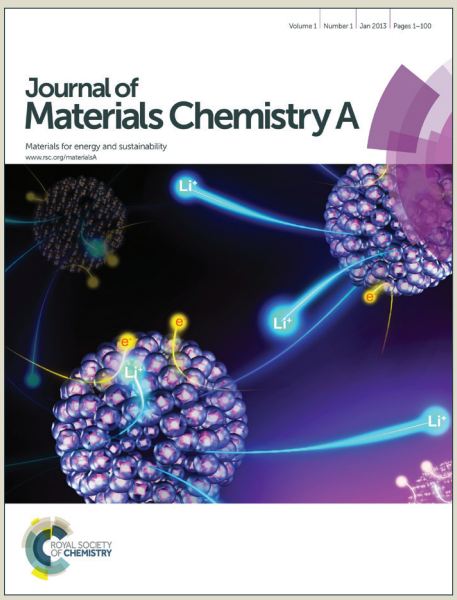

ROYAL SOCIETY OF CHEMISTRY

www.rsc.org/materialsA

Nanostructured CuP_2/C Composites as High-Performance Anode Materials for Sodium Ion Batteries

Feipeng Zhao, Na Han, Wenjing Huang, Jiaojiao Li, Hualin Ye, Fengjiao Chen, Yanguang Li*

Institute of Functional Nano & Soft Materials (FUNSOM), Soochow University, Suzhou 215123, China

E-mail: yanguang@suda.edu.cn

Abstract

Research on sodium ion batteries has recently been revived. Attention now is placed on the development of high-capacity and stable electrode materials at low costs. Among them, compounds operating on the conversion mechanism represent a promising class of anode materials. Unfortunately, they are generally plagued by poor electrical conductivity and large volume change during repeated cycling. In this study, we exploit a new type of composite materials made of copper phosphide and Super P carbon black (CuP_2/C) as potential anode candidates. The final products are consisted of crystalline CuP_2 cores coated with carbon black nanoparticles on the surface. Electrochemical measurements and multiple ex-situ studies demonstrate that CuP_2/C composites are capable of fast and reversible sodiation and desodiation based on the conversion mechanism. They deliver a large capacity in excess of 500 mAh/g, high rate capability and decent short-term cycling stability. Our study suggests that these transition metal phsophides with proper carbon coating may hold great opportunities as anode materials of sodium ion battery for effective and economical energy storage.

Introduction

Lithium ion batteries (LIBs) now have penetrated almost every corner of our society. They are widely regarded as the flagship technology for powering a wide range of applications from small portable electronic devices to large-scale grid storage.[1-2] However, there are increasing concerns about the availability of sufficient lithium resources to keep up with the ever-growing global demand.[3-4] The development of alternative technologies based on more earth-abundant elements is keenly called for.[5-6]

Over the past five years, sodium ion batteries (SIBs) have attracted revived interest.[7-10] Na^+ ions as the charge carriers share many similar electrochemical properties with Li^+ ions, both of which can diffuse into electrode materials via intercalation, alloying or conversion mechanism for effective charge storage.[7-10] For this reason, the designing principle of LIB electrode materials can be generally transplanted to aid the research on SIBs.[10] However, because of the obvious difference in the ionic radius between Na^+ and Li^+, some popular anode materials for LIBs are not suitable for SIBs. For example, the limited interlayer spacing in graphite powders precludes any significant intercalation of larger sized Na^+ ions;[8, 11] Si as a high-capacity LIB anode material cannot electrochemically alloy with Na at room temperature.[12-13] At present, the most well studied anode material for SIBs is hard carbon, which unfortunately only delivers a specific capacity in the range of 100-200 mAh/g.[14-16] Latest attention has been directed toward P, Sn and Sb.[17-20] All of them are capable of large specific capacities close to theoretic values. Nevertheless, these materials are troubled by severe pulverization as a result of the large volume change during sodiation and desodiation, resulting in poor cycling stabilities.[7]

One strategy for alleviating the pulverization problem is to utilize their compounds with

transition metals instead. Tin phosphide (Sn_4P_3), for example, has been reported by several groups as a promising SIB anode material with some success.[21-23] The presence of secondary ingredient dilutes the concentration of P species and can buffer its volume charge during repeated sodiation and desodiation. In the exploration of other transition metals to form compounds with P, we propose that Cu holds several unique advantages. Most importantly, Cu is abundantly available in the earth's crust. Its annual production is about two orders of magnitude higher than that of Sn.[24] In addition, being one of the most conductive substances known, metallic Cu nanoparticles formed upon the sodiation of Cu-P compounds can serve as the highly conductive electronic channel to enable fast electrochemical alloying of P with Na^+. Thus motivated, we report here for the first time the preparation and evaluation of CuP_2 and carbon black (CuP_2/C) composites as a potential SIB anode material with large specific capacity, decent rate capability and cycling performance.

Experimental Section

Synthesis of CuP_2/C composites: Composite materials were prepared by a two-step high energy ball milling method under the protection of Ar. In the first step, 0.76 g of copper powder and 0.74 g red phosphorus were thoroughly mixed, and milled together with ~30 g of stainless steel balls at 400 rpm for 30 h. Resulting CuP_2 powders were then mixed with Super P carbon black in 7:3 weight ratio, and balled milled for another 8 h.

Material characterizations: Scanning electron microscopy (SEM) images were taken from Zeiss scanning electron microscope. Transmission electron microscopy (TEM) images were recorded on FEI Tecnai F20 transmission electron microscope. X-ray photoelectron spectroscopy (XPS) was carried out using ULTRA DLD spectrometer. Raman spectra of dried powder samples were taken on

a Renishaw in Via plus Raman microscope with 613 nm wavelength laser excitation under 1 mV power. X-ray diffraction (XRD) was performed on PANalytical X-ray diffractometer at a scan rate of 0.05^{o}/s. For ex-situ XRD studies of electrode materials at different charge/discharge stages, battery electrodes were recovered from coin cells, quickly washed with acetone and ethanol successively, and then sealed by a thin polyethylene (PE) film before subjected to XRD measurements.

Electrochemical measurements: To prepare battery electrodes, CuP_2/C slurry was first prepared by dispersing 70 wt% of active material, 15 wt% of carbon black additive and 15 wt% polyacrylic acid polymer binder in water. It was then uniformly cast onto a Cu foil and vacuum dried at 65^{o}C overnight. The loading density of active material was ~1 mg/cm^2. 2032 type coin cells were fabricated in an Ar-filled glove box by assembling the CuP_2/C electrode with a piece of Na foil, separated by a Celgard 2400 polypropylene membrane. The electrolyte was 1 M $NaClO_4$ in ethylene carbonate (EC) and diethyl carbonate (DEC) (1:1 v/v) with 8 vol% fluoroethylene carbonate (FEC) additive. Galvanostatic charge/discharge tests were conducted in a voltage range of 0.01~2.5 V at different current rates on a MTI Battery Testing System. In addition, cyclic voltammetry curves were collected on CHI 660E potentiostat at a scan rate of 0.05 mV/s.

Results and Discussion

CuP_2/C composites were prepared by a two-step high-energy ball milling (HEBM) method as shown by Figure 1a. HEBM is widely used as a green, simple, and continuous industrialized method to prepare a variety of alloys and ceramics.[25-26] In the first step, CuP_2 compounds were prepared by milling stoichiometric amounts of metallic Cu powders and P powders under the protection of Ar for 30 hours. Obtained material was then mixed with Super P carbon black in a mass ratio of 7:3, and

further subjected to HEBM for another 8 h (see experimental details). Using this preparation method, we were able to prepare target composite materials in gram scale with high reproducibility.

Figure 1b illustrates the x-ray diffraction (XRD) patterns of CuP_2 from the first step and final CuP_2/C composites. All the diffraction peaks are in a perfect agreement with monoclinic P21/c CuP_2 (JCPDS NO. 76-1190) without Cu or P residues. The chemical reaction between Cu and P was driven to completion by the mechanical energy supplied from HEBM. Interestingly, raising the starting Cu to P molar ratio from 0.5 to 3 results in a different chemical phase attributable to Cu_3P (Supporting Information Figure S1). Formation of CuP_2/C composites is directly manifested by Raman spectra. CuP_2/C exhibits vibration modes characteristic to CuP_2 in the range of 200–500 cm^{-1}, as well as pronounced D and G bands from carbon (Figure 1c). X-ray photoelectron spectroscopy (XPS) data (Supporting Information Figure S2) suggests that both Cu and P in CuP_2 have a nominal oxidation state close to zero, which is concerted with previous observations for Cu_3P.[27] It is notable that the absolute intensity of both Cu and P signals for CuP_2/C is attenuated compared to pure CuP_2, probably owing to the surface coating with carbon black.

Furthermore, the microstructure of CuP_2/C composite was interrogated using electron microscopy. Under scanning electron microscopy (SEM), CuP_2/C was found to comprise of sub-micron sized particles (Figure 2a). Their sizes are significantly reduced compared to starting Cu and P powders (Supporting Information Figure S3). Transmission electron microscopy (TEM) reveals that the surfaces of these sub-micron sized particles are richly coated with smaller carbon black nanoparticles about 30-50 nm large (Figure 2b). From high resolution TEM (HRTEM) examination, it is evident that the primary particle has a crystalline core with clear lattice fringes corresponding to the (111) plane of CuP_2 (Figure 2c), surrounded by an amorphous surface layer

about 2-5 nm thick which is believed to be carbon. Elemental mapping under scanning transmission electron microscopy (STEM) in Figures 2d-g depicts the high spatial correlation in the distribution between Cu and P species, and therefore corroborates the formation of single-phase compound. By contrast, the distribution of C is unveiled to be more concentrated on particle surface. This result is in line with the coating of carbon black nanoparticles on the surface of primary CuP_2 particles. Such a carbon coating layer only enhances the electrical conductivity of the composite materials, but also serves as a cushion to buffer the volume change of electrode material during electrochemical sodiation/desodiation as will be discussed in what follows.

The electrochemical performance of CuP_2/C composites was evaluated in 2032 type coin cells by pairing the active materials with Na metal disks in 1:1 (v/v) ethylene carbonate (EC): diethylene carbonate (DEC) electrolyte containing 1 M $NaClO_4$ and 8 vol% fluoroethylene carbonate (FEC) additive. Their cyclic voltammetry (CV) curves were first collected and presented in Figure 3a. During the initial cathodic sweep, there was a broad reduction wave in the potential range of 1.5-0.5 V (vs. Na^+/Na, and the same hereafter), which corresponds to the irreversible decomposition of electrolyte and the formation of solid electrolyte interface (SEI) on fresh electrode surface.[22] When swept negative to 0.5 V, the cathodic current density further rose continuously, indicative of electrochemical sodiation of CuP_2/C electrode in this low potential regime. In the ensuing anodic sweep, two pronounced anodic waves centered at 0.67 and 0.88 V were observed as a result of multi-step desodiation process. CV curve from the subsequent cycle resembled that of the initial cycle but was devoid of SEI contribution. We next carried out galvanostatic charge/discharge experiments. Figure 3b depicts the voltage profiles of CuP_2/C between 0.01-2.5 V at a current density of 150 mA/g. Consistent with CV results, the initial discharge was featured with a short

plateau around 1.3 V as a result of SEI formation, followed by a long sloping region down to 0.01 V corresponding to the sodiation of CuP_2. Its specific capacity from the first discharge reached ~700 mAh/g (normalized to mass of CuP_2/C composite), but only ~470 mA/g was recovered when the electrode was fully recharged.

To gain more insights about the reaction mechanism, we disassembled coin cells at different charge/discharge stages, and tracked the composition evolution of electrode materials using XRD. As shown in Figure 4a, the primary diffraction peak of CuP_2 at ~30.9^o gradually diminished during discharge, and completely vanished when fully discharged. This process was accompanied by the emergence of a new peak at 37.2^o indexable to the (110) or (103) plane of Na_3P. Upon recharge, above composition change was reversed. The diffraction peak of CuP_2 reappeared despite that it was weaker and broader than the initial state. Such reversibility was maintained even after extended cycling (Supporting Information Figure S4). HRTEM examination of the fully discharged sample clearly evidences the formation of a large number of ~5 nm dark contrast nanoparticles densely dispersed in a light-contrast matrix (Figure 4b). From their lattice fringes, we determined that they were metallic Cu nanoparticles (Figure 4c). Some of these nanoparticles were found to be interconnected and form penetrating conductive networks. Successful sodiation of CuP_2 was also manifested by the elemental mapping of the discharged electrode as shown in Figures 4d-g. It exhibits strong Na signal, which has a spatial distribution in good accordance with those of Cu and P. HRTEM analysis of fully recharged sample shows that most of these Cu nanoparticles vanish upon recharge (Supporting Information Figure S5). Taken together, above observations led us to believe that that metallic Cu and Na_3P are the primary discharge products, and that the reversible sodiation/desodiation of CuP_2 very likely proceeds via the following conversion mechanism: CuP_2 +

$6Na^+ + 6e^- \leftrightarrows 2Na_3P + Cu$. It is worth noting that this proposed reaction mechanism is similar to that for Sn_4P_3,[21] with the only difference being that Sn can further react with Na^+ to form alloys whereas Cu stays as metallic nanoparticles at discharge. These Cu nanoparticles form conducting pathways, which might enable fast electron transport across the electrode and thus greatly facilitate battery reactions.

After having established their reversible electrochemistry, we further assessed the rate capability of CuP_2/C composites at different current densities. When both charge and discharge current rates were raised stepwise, the measured specific capacity gradually decreased from 550 mAh/g at 50 mA/g to 420 mAh/g, 325 mAh/g, 261 mAh/g and 178 mAh/g at 200 mA/g, 500 mA/g, 1000 mA/g and 2000 mA/g, respectively (Figure 5a). As the current density reverted back to 50 mA/g, a specific capacity of 470 mAh/g was recovered. The large specific capacity under high current rates surpassed most carbonaceous anode materials,[28-30] and was also well comparable to previously reported Sn_4P_3.[21-23] Moreover, even though fast charging is desirable and tempting, in practical applications the charging rate of batteries at the pack level seldom passes 1C due to safety considerations. Charging full batteries corresponds to the sodiation of anode materials. In light of this, we also evaluated the performance of CuP_2/C under small constant sodiation current density of 50 mA/g and varying desodiation current densities. As shown in Figure S6, the measured specific capacity was significantly improved, particularly under large desodiation current densities. For example, 350 mAh/g was retained even at 2000 mA/g. This underlines the potential of CuP_2/C anode materials for future high power applications.

Another important criterion in the evaluation of battery electrode materials is their cycling stability. Electrode materials based on conversion or alloying mechanism are generally more

susceptible to large volume change and thus are plagued by poor capacity retention during repeated cycling.[7, 31] Indeed, just like most other P-based electrode materials, we found that pure CuP_2 was subjected to rapid capacity decay from over 500 mAh/g to less than 50 mAh/g in about 10 cycles (Figure 5b). Balling milling with carbon black powders affords CuP_2 particles with carbon coating layer, which not only provides good electric conductivity to the electrode materials as evidenced by the reduced charge transfer resistance from electrochemical impedance spectrum (Supporting Information Figure S7), but more importantly alleviates the volume change of CuP_2. As illustrated in Figure 5b, at a charge/discharge current density of 150 mA/g, our CuP_2/C composites demonstrate high coulombic efficiency close to 100% and good cycling performance with ~430 mAh/g retained by the end of 30 cycles. This result clearly highlights the contribution of carbon coating to the success of composites. Furthermore, we also compared the performance of composites with different CuP_2 to C weight ratios and concluded that 7:3 ratio had the optimal overall performance (Supporting Information Figure S8). Less carbon in the composite led to inferior capacity retention while too much carbon resulted in smaller capacity.

Albeit of its impressive short-term cycling stability, CuP_2/C composites still lack satisfactory long-term cycling stability. Extended charge/discharge cycling of the electrode was found to result in a gradual loss of its specific capacity (Supporting Information Figure S9). To understand the origin of its failure, we examined the electrode material after 70 cycles and noticed that the electrode material had a distinctly different microstructure under SEM and TEM. In contrast to solid sub-micron sized particles observed at the initial state, materials after extended cycling exhibited roughened surfaces and highly porous interior. Even though EDX analysis still detected C signal throughout the electrode material, it appeared that the original carbon black surface coating was

mostly detached from CuP_2 particles. These results were probably indicative of material pulverization as the primary reason of unsatisfactory long-term cycling stability. Further improvements of CuP_2/C composites should focus on designing better carbon coating layers to more effectively suppress volume change of CuP_2 active materials.

Conclusions

In summary, we prepared nanostructured CuP_2/C composites using a facile high energy ball milling method. Final products were comprised of sub-micron sized CuP_2 particles coated with Super-P carbon black on the surface. The presence of carbon black coating layer not only enhanced the electrical conductivity of the composites, but also buffered the volume change of active materials. As a result, the composite electrode materials exhibited large specific capacity of >500 mAh/g and good rate capability. Ex-situ XRD and TEM studies of reaction products at different charge/discharge stages corroborated the reversible conversion mechanism from CuP_2 to Cu and Na_3P, and vice verse. Importantly, it was believed that such metallic Cu nanoparticles formed at intermediate stages provided a highly conductive electronic channel to enable fast electrochemical reaction. Moreover, the composite electrode materials demonstrated decent short-term cycling stability but were still short on long-term cycling stability. Given its low cost and ease of preparation, CuP_2/C composites represent a promising anode material for future sodium ion batteries.

Acknowledgements

We acknowledge supports from the National Natural Science Foundation of China (51472173 and 51522208), the Natural Science Foundation of Jiangsu Province (BK20140302 and

SBK2015010320), Jiangsu Key Laboratory for Carbon-Based Functional Materials and Devices, the Priority Academic Program Development of Jiangsu Higher Education Institutions and Collaborative Innovation Center of Suzhou Nano Science and Technology.

References

1. J. M. Tarascon and M. Armand, *Nature*, 2001, **414**, 359-367.
2. B. Dunn, H. Kamath and J. M. Tarascon, *Science*, 2011, **334**, 928-935.
3. G. M. Clarke, *Chem. Eng. Prog.*, 2013, **109**, 44-52.
4. http://www.meridian-int-res.com/Projects/Lithium_Problem_2.pdf.
5. Z. Yang, J. Zhang, M. C. W. Kintner-Meyer, X. Lu, D. Choi, J. P. Lemmon and J. Liu, *Chem. Rev.*, 2011, **111**, 3577-3613.
6. Y. G. Li and H. J. Dai, *Chem. Soc. Rev.*, 2014, **43**, 5257-5275.
7. N. Yabuuchi, K. Kubota, M. Dahbi and S. Komaba, *Chem. Rev.*, 2014, **114**, 11636-11682.
8. M. D. Slater, D. Kim, E. Lee and C. S. Johnson, *Adv. Funct. Mater.*, 2013, **23**, 947-958.
9. V. Palomares, P. Serras, I. Villaluenga, K. B. Hueso, J. Carretero-Gonzalez and T. Rojo, *Energy Environ. Sci.*, 2012, **5**, 5884-5901.
10. S. W. Kim, D. H. Seo, X. H. Ma, G. Ceder and K. Kang, *Adv. Energy Mater.*, 2012, **2**, 710-721.
11. P. Ge and M. Fouletier, *Solid State Ionics*, 1988, **28-30**, 1172-1175.
12. L. D. Ellis, B. N. Wilkes, T. D. Hatchard and M. N. Obrovac, *J. Electrochem. Soc.*, 2014, **161**, A416-A421.
13. S. C. Jung, D. S. Jung, J. W. Choi and Y.-K. Han, *J. Phys. Chem. Lett.*, 2014, **5**, 1283-1288.
14. V. L. Chevrier and G. Ceder, *J. Electrochem. Soc.*, 2011, **158**, A1011-A1014.
15. S. Komaba, W. Murata, T. Ishikawa, N. Yabuuchi, T. Ozeki, T. Nakayama, A. Ogata, K. Gotoh and K. Fujiwara, *Adv. Funct. Mater.*, 2011, **21**, 3859-3867.
16. D. A. Stevens and J. R. Dahn, *J. Electrochem. Soc.*, 2000, **147**, 1271-1273.
17. L. Wu, X. H. Hu, J. F. Qian, F. Pei, F. Y. Wu, R. J. Mao, X. P. Ai, H. X. Yang and Y. L. Cao, *Energy Environ. Sci.*, 2014, **7**, 323-328.
18. J. F. Qian, X. Y. Wu, Y. L. Cao, X. P. Ai and H. X. Yang, *Angew. Chem., Int. Ed.*, 2013, **52**, 4633-4636.
19. Y. H. Xu, Y. J. Zhu, Y. H. Liu and C. S. Wang, *Adv. Energy Mater.*, 2013, **3**, 128-133.
20. Y. J. Zhu, X. G. Han, Y. H. Xu, Y. H. Liu, S. Y. Zheng, K. Xu, L. B. Hu and C. S. Wang, *Acs Nano*, 2013, **7**, 6378-6386.
21. Y. Kim, Y. Kim, A. Choi, S. Woo, D. Mok, N. S. Choi, Y. S. Jung, J. H. Ryu, S. M. Oh and K. T. Lee, *Adv. Mater.*, 2014, **26**, 4139-4144.
22. W. J. Li, S. L. Chou, J. Z. Wang, J. H. Kim, H. K. Liu and S. X. Dou, *Adv. Mater.*, 2014, **26**, 4037-4042.
23. J. F. Qian, Y. Xiong, Y. L. Cao, X. P. Ai and H. X. Yang, *Nano Lett.*, 2014, **14**, 1865-1869.
24. https://en.wikipedia.org/wiki/Abundance_of_elements_in_Earth%27s_crust.
25. S. Indris, D. Bork and P. Heitjans, *J. Mater. Synth. Process.*, 2000, **8**, 245-250.
26. T. P. Yadav, R. M. Yadav and D. P. Singh, *Nanosci. Nanotechnol.*, 2012, **2**, 22-48, 27 pp.

27. J. Q. Tian, Q. Liu, N. Y. Cheng, A. M. Asiri and X. P. Sun, *Angew. Chem., Int. Ed.*, 2014, **53**, 9577-9581.
28. Y. L. Cao, L. F. Xiao, M. L. Sushko, W. Wang, B. Schwenzer, J. Xiao, Z. M. Nie, L. V. Saraf, Z. G. Yang and J. Liu, *Nano Lett.*, 2012, **12**, 3783-3787.
29. K. Tang, L. J. Fu, R. J. White, L. H. Yu, M. M. Titirici, M. Antonietti and J. Maier, *Adv. Energy Mater.*, 2012, **2**, 873-877.
30. Y. Wen, K. He, Y. J. Zhu, F. D. Han, Y. H. Xu, I. Matsuda, Y. Ishii, J. Cumings and C. S. Wang, *Nat. Commun.*, 2014, **5**.
31. F. Klein, B. Jache, A. Bhide and P. Adelhelm, *Phys. Chem. Chem. Phys.*, 2013, **15**, 15876-15887.

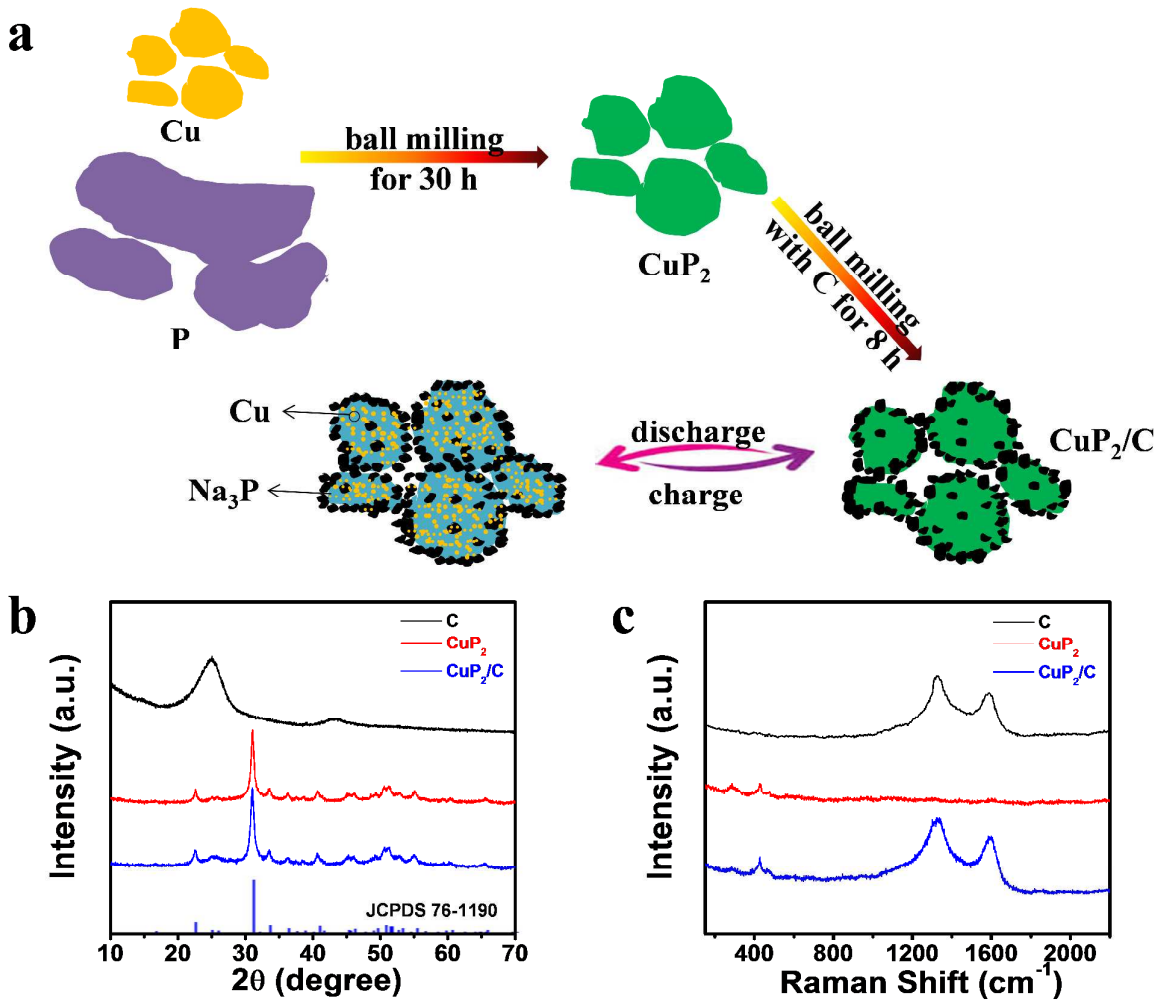

Figure 1. (a) A schematic illustration of the general synthetic procedure of nanostructured CuP_2/C composites and their structure evolution during electrochemical charge and discharge; (b) XRD patterns and (c) Raman spectra of Super P carbon black, pure CuP_2 and CuP_2/C composites.

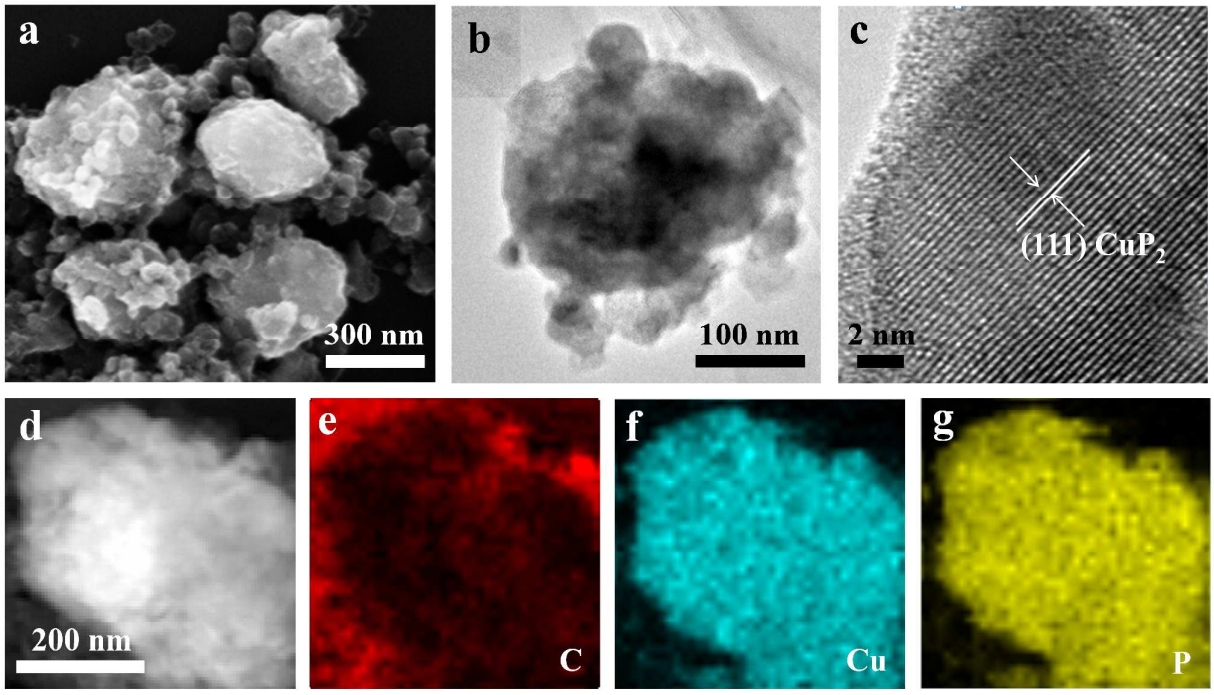

Figure 2. Electron microscopy studies of CuP_2/C composites. (a) SEM image; (b-c) TEM images; (d) STEM image and (e-g) corresponding EDS mapping of constituent elements.

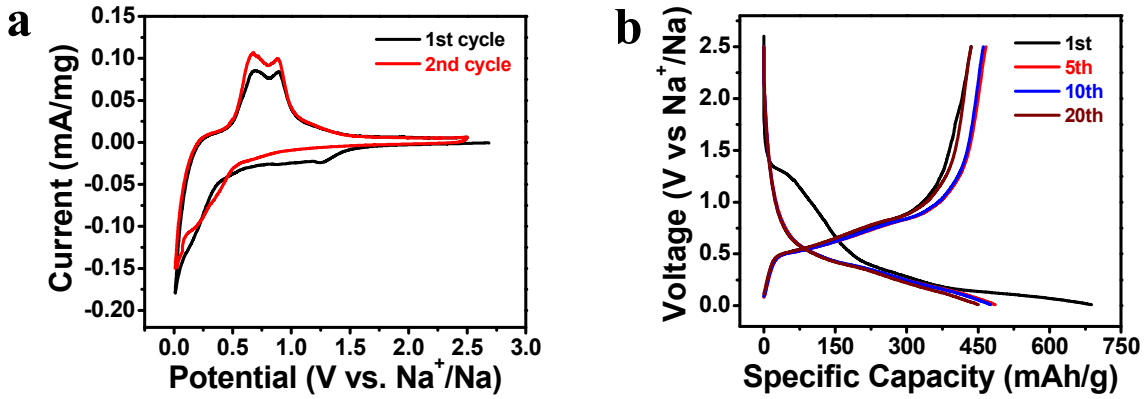

Figure 3. (a) CV curve of CuP_2/C for the first two cycles at a scan rate of 0.05 mV/s; (b) representative galvanostatic charge/discharge curves of CuP_2/C at 150 mA/g.

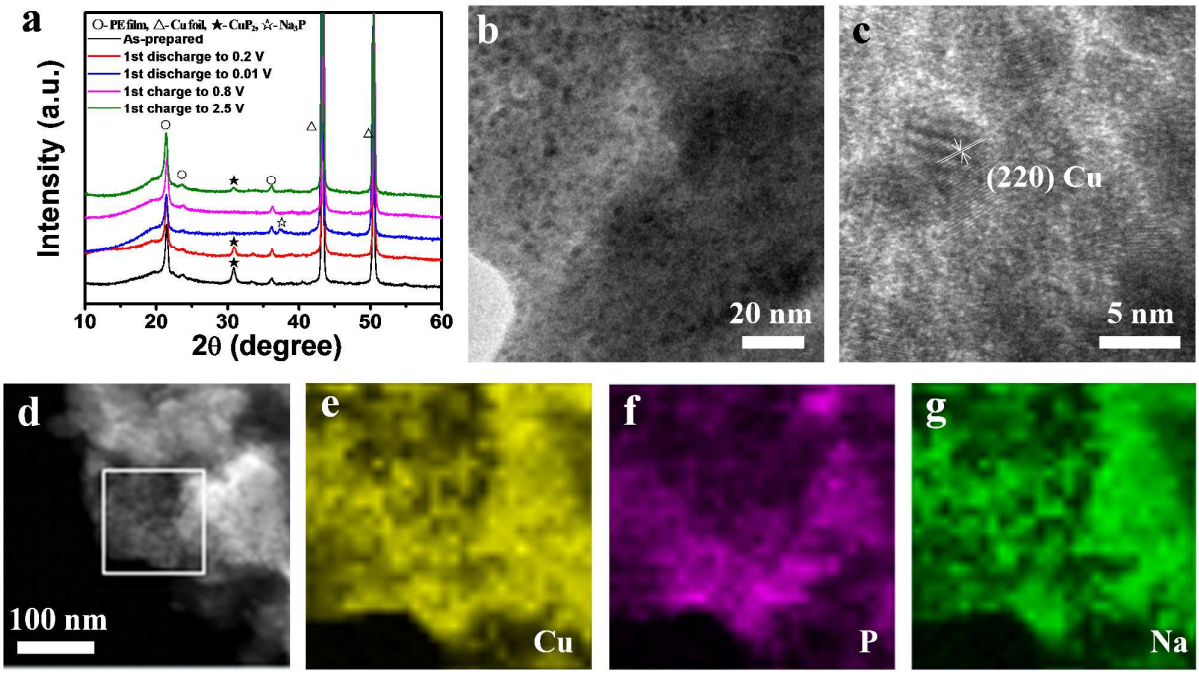

Figure 4. (a) XRD patterns of CuP_2/C electrode materials at different charge/discharge stages as indicated; (b-c) TEM images of fully discharged material, (d) STEM image and (e-f) corresponding EDS elemental mapping of fully discharged material. These data suggest successful sodiation and desodiation of CuP_2.

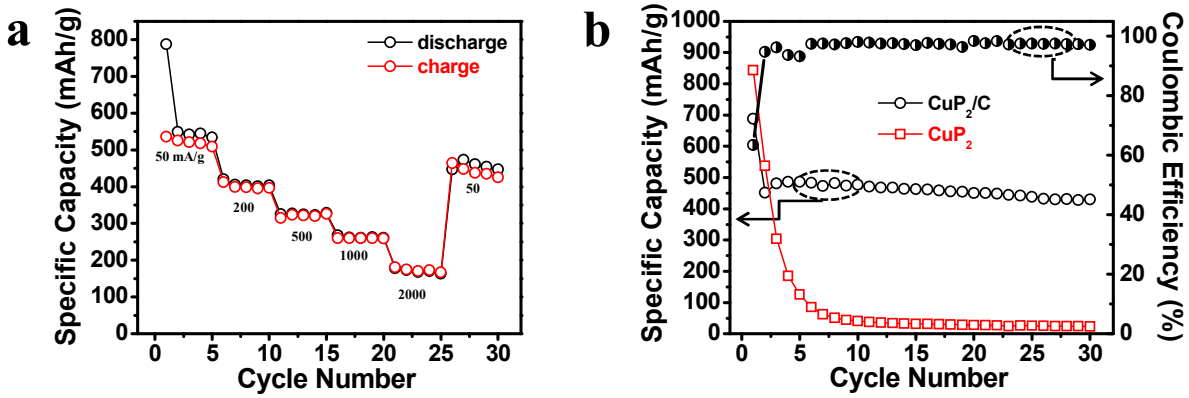

Figure 5. (a) Rate capability of CuP_2/C electrode materials under varying current densities as indicated; (b) cycling performance and coulombic efficiency of CuP_2/C at 150 mAh/g.

TOC

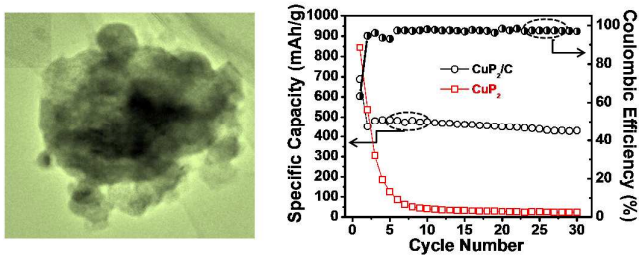

CuP_2/C composites from high energy ball milling demonstrate potential as the anode material of sodium ion batteries.